CHEMISTRY
A EUROPEAN JOURNAL

DOI: 10.1002/chem.200601792

How ^{77}Se NMR Chemical Shifts Originate from Pre-α, α, β, and γ Effects: Interpretation Based on Molecular Orbital Theory

Waro Nakanishi,*[a] Satoko Hayashi,[a] and Masahiko Hada[b]

Abstract: Plain rules founded in a theoretical background are presented that can be used to determine the structure of selenium compounds on the basis of δ(Se) data and to predict δ(Se) data from a given structure with satisfactory accuracy. As a first step to establish such rules, the origin of δ(Se) is elucidated on the basis of MO theory. The Se^{2-} ion was chosen as the standard for the analysis. The concept of the pre-α effect is proposed, which is defined as the downfield shift due to protonation of a lone-pair orbital of Se. The pre-α effect of two protons in H_2Se is explained by the generation of double σ(Se–H) and σ*(Se–H) through protonation of the spherical Se^{2-} ion. The orbitals, together with n_p(Se), result in effective transitions for the pre-α effect. The α effect is the downfield shift caused by the replacement of Se–H by Se–Me. The extension of HOMO−2 [$4p_y$(Se)], HOMO−1 [$4p_x$(Se)], and HOMO [$4p_z$(Se)] over the whole Me_2Se molecule is mainly responsible for the α effect. The β effect originates not from the occupied-to-unoccupied ($\psi_i \rightarrow \psi_a$) transitions but from the occupied-to-occupied ($\psi_i \rightarrow \psi_j$) transitions. Although $\psi_i \rightarrow \psi_j$ transitions contribute to upfield shifts in Me_2Se, the magnitudes become smaller as the methyl protons are substituted by Me groups one after another. The γ effect of upfield shifts is also analyzed, although complex. The effect of p(Se)–π(C=C) conjugation is analyzed in relation to the orientational effect. Contributions from each MO (ψ_i) and each $\psi_i \rightarrow \psi_a$ transition are evaluated separately, by using a utility program derived from the Gaussian 03 program suite (NMRANAL-NH03G). The treatment enables us to visualize and understand the origin of ^{77}Se NMR chemical shifts.

Keywords: ab initio calculations · ligand effects · NMR spectroscopy · selenium

Introduction

Nuclear magnetic resonance spectroscopy is one of most powerful tools in chemistry:[1] NMR spectra are measured and analyzed on a daily basis to determine structures with the guidance of empirical rules.[2] ^{77}Se NMR chemical shifts δ(Se) are also widely used to follow reactions, since they are highly sensitive to structural changes in selenium compounds.[2–5] Although empirical rules are useful for assigning spectra, it is difficult to understand the origin of chemical shifts on the basis of such rules. It is still difficult to predict chemical shifts for a given structure with satisfactory accuracy by using empirical rules. Experimental chemists need plain rules founded in theory which can be used to determine the structure of selenium compounds on the basis of δ(Se). With such rules, the relationship between chemical shifts and electronic structures could be considered for unknown compounds, and such considerations could create new ideas. We investigated selenium compounds by ^{77}Se NMR spectroscopy and tried to understand δ(Se) of organic selenium compounds from a theoretical point of view. We noted the importance of the orientational effect of the Ar group on δ(Se) in ArSeR, and proposed a mechanism for understanding δ(Se) of ArSeR in a uniform manner.[6,7]

The dependence of δ(Se) of selenium compounds on respective structure is elucidated here for various selenides on the basis of MO theory, as a first step in establishing rules founded on the theoretical principles. Our aim is to enable experimental chemists to understand the origin of these chemical shifts. To this end, a concept called the "pre-α effect" is proposed for better understanding of δ(Se). The

[a] Prof. Dr. W. Nakanishi, Dr. S. Hayashi
Department of Material Science and Chemistry
Faculty of Systems Engineering, Wakayama University
930 Sakaedani, Wakayama 640-8510 (Japan)
Fax: (+81) 73-457-8253
E-mail: nakanisi@sys.wakayama-u.ac.jp

[b] Prof. Dr. M. Hada
Department of Chemistry
Faculty of Graduate School of Science and Engineering
Tokyo Metropolitan University
1–1 Minami-osawa, Hachioji-shi, Tokyo 192-0397 (Japan)

Supporting information for this article is available on the WWW under http://www.chemeurj.org/ or from the author.

pre-α effect is defined as the downfield shift due to addition of a proton to a lone pair orbital of Se, as shown in Scheme 1. For example, the δ(Se) value of H_2Se δ(Se: H_2Se) relative to Se^{2-} corresponds to twice the pre-α effect. The α and β effects[3b,8] are well known as the downfield shifts in the respective processes leading, for instance, from H_2Se to MeSeH and then to EtSeH. The mechanisms of the pre-α, α, and β effects are elucidated. The γ effect of upfield shifts is also discussed, together with its mechanism, which corresponds to the process leading from EtSeH to *n*PrSeH, for example.[3b,8] The δ effect in *n*BuSeR relative to *n*PrSeR is also mentioned, although its magnitude is negligible. The effect of p(Se)–π(C=C) conjugation[9] involving ethenyl and phenyl groups is analyzed together with its mechanism, in relation to the orientational effect.[7]

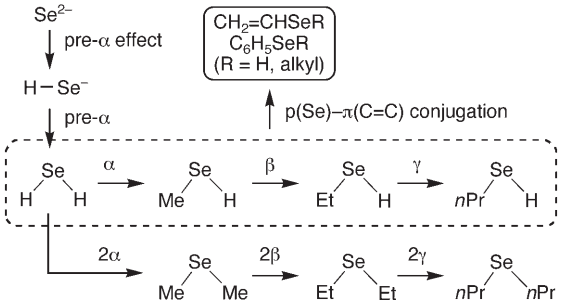

Scheme 1. Pre-α, α, β, and γ effects, as well as the effect of p(Se)–π(C=C) conjugation.

It is informative to employ the total absolute magnetic shielding tensors $\boldsymbol{\sigma}^t$ for the analysis of δ(Se), since $\boldsymbol{\sigma}^t$ can be predicted with satisfactory accuracy. The $\boldsymbol{\sigma}^t$ are decomposed into diamagnetic ($\boldsymbol{\sigma}^d$) and paramagnetic ($\boldsymbol{\sigma}^p$) contributions [Eq. (1)].[10–12] The magnetic shielding tensors consist of three components, exemplified for $\boldsymbol{\sigma}^p$ in Equation (2). Since $\boldsymbol{\sigma}^p$ is evaluated by the coupled Hartree–Fock (CPHF) method, it can be decomposed into the contributions of the occupied orbitals or orbital–orbital transitions[13] [Eq. (3)]. $\boldsymbol{\sigma}^d$ is expressed simply as the sum of contributions over the occupied orbitals (ψ_i), as shown in Equation (4).

$$\boldsymbol{\sigma}^t = \boldsymbol{\sigma}^d + \boldsymbol{\sigma}^p \quad (1)$$

$$\boldsymbol{\sigma}^p = (\boldsymbol{\sigma}^p_{xx} + \boldsymbol{\sigma}^p_{yy} + \boldsymbol{\sigma}^p_{zz})/3 \quad (2)$$

$$\boldsymbol{\sigma}^p = \sum_i^{occ} \sum_a^{unocc} \boldsymbol{\sigma}^p_{i\rightarrow a} = \sum_i^{occ} \boldsymbol{\sigma}^p_i \quad (3)$$

$$\boldsymbol{\sigma}^d = \sum_i^{occ} \boldsymbol{\sigma}^d_i \quad (4)$$

While $\boldsymbol{\sigma}^p$ is evaluated accurately by the CPHF method and decomposed by Equation (3),[14] we will mainly discuss $\boldsymbol{\sigma}^p$ with an approximated image derived from Equation (5).[15] Since $\boldsymbol{\sigma}^p_{zz,N}$ contains the $\hat{L}_{z,N}$ operator, $\boldsymbol{\sigma}^p_{zz,N}$ arises from admixtures between atomic p_x and p_y orbitals of *N* in various molecular orbitals when a magnetic field is applied. Admixtures of unoccupied molecular orbitals (ψ_a, ψ_b,...) into occupied molecular orbitals (ψ_i, ψ_j,...) mainly contribute to $\boldsymbol{\sigma}^p_{zz,N}$,[13] if ψ_i and ψ_a contain $p_x(N)$ and $p_y(N)$, for example. $\boldsymbol{\sigma}^p_{xx,N}$ and $\boldsymbol{\sigma}^p_{yy,N}$ are understood similarly.

$$\boldsymbol{\sigma}^p_{zz,N} = -(\mu_o e^2/2m_e^2) \sum_i^{occ} \sum_a^{unocc} (\varepsilon_a - \varepsilon_i)^{-1} \times \{\langle\psi_i|\hat{L}_z|\psi_a\rangle\langle\psi_a|\hat{L}_{z,N} r_N^{-3}|\psi_i\rangle + \langle\psi_i|\hat{L}_{z,N} r_N^{-3}|\psi_a\rangle\langle\psi_a|\hat{L}_z|\psi_i\rangle\} \quad (5)$$

A utility program derived from Gaussian 03 (NMRANAL-NH03G) was applied to evaluate the contributions separately from each MO (ψ_i) and each $\psi_i \rightarrow \psi_a$ transition.[16] The utility program visualizes the process by which δ(Se) arises, and this helps us to understand the origin of δ(Se).[7]

Results and Discussion

Calculation method: Structures were optimized by employing the 6-311+G(3df) basis set for Se and the 6-311+G(3d,2p) basis set for other nuclei in the Gaussian 03 program package.[17] Structural optimization was performed at the DFT level of the Becke three-parameter hybrid functional with Lee–Yang–Parr correlation functional (B3LYP).[18] The gauge-independent atomic orbital (GIAO) method[19] was applied to evaluate absolute magnetic shielding tensors of Se [$\boldsymbol{\sigma}$(Se)] at the DFT (B3LYP) level on structures optimized with the same basis sets (GIAO-DFT method). Here $\boldsymbol{\sigma}$(Se) is used in place of $\boldsymbol{\sigma}_{Se}$ in Equation (5), in analogy to δ(Se).

The Möller–Plesset second-order energy correlation (MP2) method[20] was also applied to evaluate $\boldsymbol{\sigma}^t$(Se) with the same basis sets as in the GIAO-DFT method, employing the optimized structures at the DFT level, for convenience of comparison. This is called the GIAO-MP2 method here. The $\boldsymbol{\sigma}^p$(Se) are mainly employed to discuss δ(Se) of selenium compounds, since $\boldsymbol{\sigma}^p$(Se) are sharply sensitive to structural changes in selenium compounds.

Standard of σ(Se) for analysis: To analyze and understand the observed δ(Se) on the basis of MO theory, a suitable standard (the simpler the better) for σ(Se) was searched for. The electronic state of the selenium atom is $^3P_2$, which is unsuitable for a standard, since it is not the singlet state. Therefore, $\boldsymbol{\sigma}^d$(Se), $\boldsymbol{\sigma}^p$(Se), and $\boldsymbol{\sigma}^t$(Se) of neutral and charged Se in the singlet state were calculated with the GIAO-DFT method. Table 1 lists the results, together with $\boldsymbol{\sigma}^t$(Se) evaluated at the MP2 level for comparison.

Table 1 shows that 1) $\boldsymbol{\sigma}^d$(Se) will not contribute so much to the change in $\boldsymbol{\sigma}^t$(Se): the difference in $\boldsymbol{\sigma}^d$(Se) from Se^{4+} to Se^{2-} is predicted to be 43 ppm and 2) $\boldsymbol{\sigma}^p$(Se) contribute predominantly to $\boldsymbol{\sigma}^t$(Se). 3) The charge at Se is not main factor controlling $\boldsymbol{\sigma}^t$(Se); instead, 4) the practically occupied 4p electron distribution around Se strongly affects $\boldsymbol{\sigma}^t$(Se) through $\boldsymbol{\sigma}^p$(Se).

Table 1. Absolute shielding tensors of variously charged Se in the singlet state, calculated at the DFT and MP2 levels.[a,b]

	Configuration	σ^d(Se)[c]	σ^p(Se)[c]	σ^t(Se)[c]	σ^t(Se)[d]
Se^{6+}	$(4s)^0(4p)^0$	2937.4	0.0	2937.4	2937.3
Se^{4+}	$(4s)^2(4p)^0$	2962.6	0.0	2962.6	2962.3
Se^{2+}	$(4s)^2(4p)^2$	2981.8	21439.4	24421.3	24867.1
Se^0	$(4s)^2(4p)^4$	2996.9	18133.4	21130.3	21777.2
Se^{2-}	$(4s)^2(4p)^6$	3005.7	0.0	3005.7	3005.1

[a] Calculated with the 6-311+G(3df) basis set of Gaussian 03. [b] In ppm. [c] At the DFT (B3LYP) level. [d] At the MP2 level.

Compilation of these results led us to choose σ(Se: Se^{2-}) for the standard of σ(Se), since σ^d(Se: Se^{2-}) of 3006 ppm is very close to those for usual selenium compounds (see also Table 2) and σ^p(Se: Se^{2-}) = 0 ppm is most favorable for the standard. The $^1S_0$ electronic state of Se^{2-} with eight valence electrons according to the octet rule is also desirable, as is its spherical electron distribution.

Analysis of δ(Se) on the basis of MO theory: Axes of RSeR and RSeR′ utilized in this work are shown in Scheme 2, together with some orbitals. The direction of the p-type lone pair orbital n_p(Se) in H_2Se is set to the z axis, which is perpendicular to the molecular plane, the bisected ∢HSeH direction is set to the x axis, and that perpendicular to the two is the y axis. Axes for symmetrical selenides (RSeR) are essentially the same as those of H_2Se. However, the directions in unsymmetrical RSeR′ (R > R′) are usually different from those of H_2Se. In this case, the Se–C_R and Se–$C_{R'}$ directions are set to the y and x axes, respectively, and that of n_p(Se) is set to the z axis, if possible.

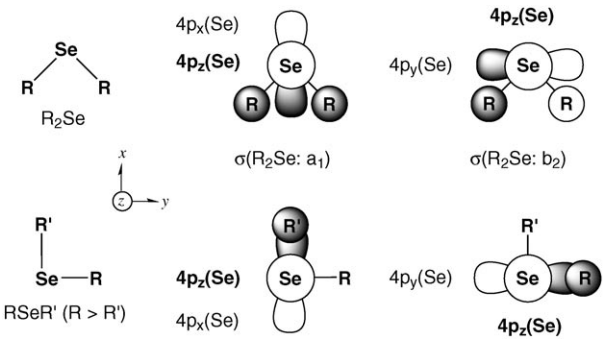

Scheme 2. Axes in RSeR and RSeR′, together with some orbitals. p-Type orbitals are used for Se and s-type for R and R′.

Table 2 lists σ^d(Se), σ^p(Se), and σ^t(Se) of various selenides calculated by the GIAO-DFT method, together with σ^t(Se) by the GIAO-DFT method.[21] The GIAO-DFT calculations usually overestimate σ^p(Se), due to the underestimation of orbital energy differences.[22] Therefore, it is instructive to examine the relationship between σ^t(Se) calculated with the GIAO-DFT method and those computed with the GIAO-MP2 method. The data given in Table 2, together with those of ethenyl and phenyl derivatives (see Table 8 below), were employed to plot σ^t(Se) with the GIAO-DFT method versus those with the GIAO-MP2 method.

Equation (6) shows the correlation, whereby the data for Se^{2-} are neglected[23,24] and n is the number of data used in the correlation. The correlation is very good (r = 0.996) with a correlation constant (a in $y = ax + b$) of 1.08. The results show that the GIAO-DFT method overestimates σ^t(Se) due to the structural change by about 8% more than the GIAO-

Table 2. Calculated pre-α, α, and β effects of various selenides, together with the observed values.[a,b]

	GIAO-DFT				GIAO-MP2		Observed		
Compound	σ^d(Se)	σ^p(Se)	σ^t(Se)	effect[c,d]	σ^t(Se)	effect[c,d]	δ(Se)	effect[d,e]	solvent
Se^{2-} (O_h)	3005.7	0.0	3005.7		3005.1				
HSe^- ($C_{\infty v}$)	3001.3	−501.2	2500.2	−505.5: pα	2628.6	−376.5: pα	−447[f]		DMF
$MeSe^-$ (C_{3v})	3000.9	−1135.8	1865.1	−635.1: α	2124.4	−504.2: α	−332[g]	115: α	H_2O
$EtSe^-$ (C_s)	3004.3	−1343.3	1661.0	−204.1: β	1929.3	−195.1: β	−150[g]	182: β	H_2O
iPrSe$^-$ (C_s)	3009.7	−1485.1	1524.6	−170.3: β	1778.6	−172.9: β	8.7[g]	170: β	H_2O
tBuSe$^-$ (C_s)	3016.2	−1586.7	1429.5	−145.2: β	1655.3	−156.4: β	129[g]	154: β	H_2O
H_2Se (C_{2v})	2998.0	−931.3	2066.7	−469.5: pα	2252.7	−376.2: pα	−331.7[h]	222: pα	GP[i]
MeSeH (C_s)	2998.2	−1155.0	1843.2	−223.5: α	2072.7	−180.0: α	−141.6[j]	111: α	GP[i]
EtSeH (C_s)	3000.1	−1235.0	1765.1	−78.1: β	1995.5	−77.2: β	36[k]	151: β	$CDCl_3$
iPrSeH (C_s)	3004.5	−1469.7	1534.8	−154.2: β	1776.2	−148.3: β	161[k]	151: β	$CDCl_3$
tBuSeH (C_s)	3009.3	−1553.5	1455.8	−129.1: β	1696.2	−125.3: β	289[k]	144: β	$CDCl_3$
Me_2Se (C_{2v})	2999.1	−1349.0	1650.1	−208.3: α	1907.4	−172.7: α	0.0[l]	115: α	$CDCl_3$
Et_2Se (C_{2v})	3006.2	−1516.6	1489.6	−80.3: β	1747.6	−79.9: β	230[k]	115: β	$CDCl_3$
iPr$_2$Se (C_2)	3015.3	−1777.1	1238.2	−103.0: β	1476.1	−107.8: β	429[k]	107: β	$CDCl_3$
tBu$_2$Se (C_2)	3027.1	−1970.7	1056.4	−99.0: β	–[m]	–[m]	614[k]	102: β	$CDCl_3$
H_3Se^+ (C_{3v})	2996.0	−1081.0	1915.0	−363.6: pα	2096.9	−302.7: pα			
MeH_2Se^+ (C_s)	2996.8	−1266.0	1730.8	−182.4: α	1945.5	−151.4: α			
EtH_2Se^+ (C_s)	2999.2	−1310.3	1688.9	−41.9: β	1903.3	−42.2: β			
Me_3Se^+ (C_3)	2997.2	−1566.1	1431.1	−161.3: α	1678.1	−229.3[n]	253[g]	253[n]	H_2O
Et_3Se^+ (C_3)	3008.5	−1698.7	1309.8	−40.4: β	1528.0	−50.0: β	377[g]	41: β	H_2O

[a] The 6-311+G(3df) basis set was employed for Se and the 6-311+G(3d,2p) basis set for other nuclei with Gaussian 03. [b] In ppm. [c] On the σ(Se) scale. [d] Values and the corresponding effects are shown. [e] On the δ(Se) scale. [f] Ref. [38]. [g] Ref. [3a]. [h] Ref. [39] and δ(Se) = −225.5 (neat).[40] [i] In the gas phase. [j] Ref. [39] and δ(Se) = −115 in $CDCl_3$.[40] [k] Ref. [40]. [l] δ(Se) = 13.1 in the gas phase.[39] [m] Not calculated due to large memory requirements. [n] Relative to Me_2Se, which corresponds to the pre-α and α effects.

MP2 method. Equation (7) exhibits the correlation for which the data for Se^{2-}, HSe^-, H_2Se, and H_3Se^+[24,25] are neglected, which corresponds to those for the derivatives of selenide anions, hydrogen selenides, selenides, and selenonium ions. The very good correlation ($a=0.995$ and $r=0.994$) implies that the GIAO-DFT method is useful for analyzing δ(Se), as well as the GIAO-MP2 method, if calculated values are carefully applied, especially for Se^{2-}, HSe^-, H_2Se, and H_3Se^+.

$$\boldsymbol{\sigma}^{t}(\mathrm{B3LYP}) = 1.084\,\boldsymbol{\sigma}^{t}(\mathrm{MP2}) - 390.8 \quad (n = 28,\ r = 0.996) \quad (6)$$

$$\boldsymbol{\sigma}^{t}(\mathrm{B3LYP}) = 0.995\,\boldsymbol{\sigma}^{t}(\mathrm{MP2}) - 233.5 \quad (n = 25,\ r = 0.994) \quad (7)$$

The typical values of the pre-α and α effects, evaluated by the GIAO-DFT method, are $\delta=-470$ and -208 ppm, respectively, which correspond to half the values of $\boldsymbol{\sigma}^t$(Se) in the processes leading from Se^{2-} to H_2Se and then to Me_2Se, respectively (Table 2). The effects are predicted to be -376 and -173 ppm, respectively, by the GIAO-MP2 method. The magnitudes at the DFT level are 1.25 and 1.20 times larger than those at the MP2 level, respectively, which correspond to the particular cases in Equation (6).[26] The β effects for EtSeH and Et_2Se are predicted to have almost the same value of -77 to -80 ppm in $\boldsymbol{\sigma}^t$(Se) with both DFT and MP2 methods (Table 2). The results are in accordance with the predictions of Equation (7).

Table 3 shows the contributions from each ψ_i of the valence orbital to $\boldsymbol{\sigma}^p$(Se) and the components $\boldsymbol{\sigma}^p(Se)_{xx}$, $\boldsymbol{\sigma}^p(Se)_{yy}$, and $\boldsymbol{\sigma}^p(Se)_{zz}$ in H_2Se, Me_2Se, and Et_2Se, together with the energies (ε_i) and the characters of ψ_i. Table 4 collects the main contributions from each $\psi_i \rightarrow \psi_a$ transition to $\boldsymbol{\sigma}^p(Se)_{xx}$, $\boldsymbol{\sigma}^p(Se)_{yy}$, and $\boldsymbol{\sigma}^p(Se)_{zz}$ in H_2Se, Me_2Se, and Et_2Se, together with the energy differences and characters of ψ_a. The data will be discussed in relation to the origin of the pre-α, α, and β effects. Tables 5 and 6 list the β and γ effects, respec-

Table 3. Contributions to $\boldsymbol{\sigma}^p$(Se) and components from ψ_i in H_2Se, Me_2Se, and Et_2Se, together with the energies and characters of ψ_i.[a–d]

i in ψ_i	ε [eV]	$\boldsymbol{\sigma}^p(Se)_{xx}$	$\boldsymbol{\sigma}^p(Se)_{yy}$	$\boldsymbol{\sigma}^p(Se)_{zz}$	$\boldsymbol{\sigma}^p$(Se)	Symmetry	Character
H_2Se							
$\psi_i \rightarrow \psi_j$		317.9	314.8	318.7	317.1		
1–14		−15.9	−5.8	−7.0	−9.6		inner orbitals
15	−19.58	−1.4	−17.0	−29.4	−15.9	A1	σ[HSe_2: 4s(Se)]
16	−11.53	−247.4	−9.6	−482.3	−246.4	B2	σ[H_2Se b_2: $4p_y$(Se)]
17	−9.86	−4.5	−215.4	−831.5	−350.5	A1	σ[H_2Se a_1: $4p_x$(Se)]
18	−6.91	−1312.4	−565.0	−0.3	−625.9	B1	$4p_z$(Se)
1–18		−1581.7	−812.9	−1350.6	−1248.4		
total		−1263.8	−498.1	−1031.9	−931.3		
Me_2Se							
$\psi_i \rightarrow \psi_j$		437.1	410.1	328.3	391.8		
1–16		10.5	30.9	53.8	31.7		inner orbitals
17–19	–[e]	−17.5	−30.1	−81.5	−43.0	–[f]	mainly 4s(Se) or σ(Me)
20	−11.90	−4.1	−8.0	−113.2	−41.8	A1	σ[$MeSe_2$: $4p_x$(Se)]
21	−11.88	−124.7	−79.8	−3.2	−69.3	B1	π[Me_2Se: $4p_z$(Se)]
22	−11.48	−3.1	−0.0	−240.5	−81.2	B2	σ[Me_2Se: $4p_y$(Se)]
23	−11.29	−3.3	−1.3	−1.9	−2.1	A2	π_z*(Me–Me)
24	−9.54	−405.0	−5.2	36.7	−124.5	B2	σ[Me_2Se b_2: $4p_y$(Se)]
25	−8.40	−8.4	−405.9	−1530.1	−648.1	A1	σ[Me_2Se a_1: $4p_x$(Se)]
26	−5.84	−1470.1	−816.8	−0.7	−762.5	B1	$4p_z$(Se)
1–26		−2025.7	−1316.2	−1880.5	−1740.8		
total		−1588.6	−906.2	−1552.2	−1349.0		
Et_2Se							
$\psi_i \rightarrow \psi_j$		−11.3	304.7	232.9	175.4		
1–18		19.1	26.2	45.5	30.3		inner orbitals
19–23	–[g]	12.2	−27.6	−69.1	−28.3	–[h]	mainly 4s(Se) or σ(Et)
24	−12.64	−53.0	−47.7	−1.7	−34.1	B1	π_z[Et_2Se: $4p_z$(Se)]
25	−12.33	−4.3	−0.5	−0.2	−1.7	A2	π_z(Et–Et)
26	−12.12	−29.6	−0.4	−90.5	−40.2	B2	σ[Et_2Se: $4p_y$(Se)]
27	−11.29	−5.2	−1.7	−1.1	−2.7	A1	σ[Et_2Se: 4s(Se)]
28	−10.79	−1.6	−33.8	−250.6	−95.4	A1	σ[Et_2Se: $4p_x$(Se)]
29	−10.28	6.1	−0.3	−38.9	−11.0	B2	σ(C–C)
30	−10.06	−91.4	−40.2	−3.0	−44.8	B1	π_z*[Et_2Se: $4p_z$(Se)]
31	−9.75	−3.1	−1.0	−4.2	−2.8	A2	π_z*(Et–Et)
32	−8.69	−182.0	−3.1	−258.2	−147.8	B2	σ(Et_2Se b_2: $4p_y$(Se))
33	−8.06	−4.6	−300.3	−1314.5	−539.8	A1	σ(Et_2Se a_1: $4p_x$(Se))
34	−5.74	−1537.3	−783.8	−0.6	−773.9	B1	$4p_z$(Se)
1–34		−1874.9	−1214.1	−1987.0	−1692.0		
total		−1886.3	−909.4	−1754.1	−1516.6		

[a] Optimized with the 6-311+G(3df) basis set for Se and 6-311+G(3d,2p) basis set for other nuclei from Gaussian 03. [b] A utility program of Gaussian 03 (NMRANAL-NH03G) was applied to separate the contributions from each molecular orbital. [c] The contribution from each molecular orbital contains only that from the $\psi_i \rightarrow \psi_a$ transitions. [d] $\boldsymbol{\sigma}$(Se) and the components are given in ppm. [e] −20.95 to −16.30 eV. [f] Symmetries are A1, B2, and A1 for i=17–19, respectively. [g] −21.61 to −15.77 eV. [h] Symmetries are A1, B2, A1, B2, and A1 for i=19–23, respectively.

Table 4. Contributions from $\psi_i \rightarrow \psi_a$ transitions to $\sigma^p(Se)_{xx}$, $\sigma^p(Se)_{yy}$, and $\sigma^p(Se)_{zz}$ in H_2Se, Me_2Se, and Et_2Se, together with the energy differences and characters of ψ_a.[a–c]

$\psi_i \rightarrow \psi_a$	$\Delta\varepsilon$ [eV]	$\sigma^p(Se)_{xx}$	$\sigma^p(Se)_{yy}$	$\sigma^p(Se)_{zz}$	Character of ψ_a
H_2Se[d]					
16(B2)→24(A1)	13.31	0	0	−164	σ*[H_2Se a_1: $4p_x$(Se)]
17(A1)→20(B2)	9.62	0	0	−581	σ*[H_2Se b_2: $4p_y$(Se)]
17(A1)→32(B2)	18.74	0	0	−150	σ*[H_2Se b_2: $5p_y$(Se)]
18(B1)→19(A1)	6.28	0	−255	0	σ*[H_2Se a_1: $4p_x$(Se)]
18(B1)→20(B2)	6.67	−1251	0	0	σ*[H_2Se b_2: $4p_y$(Se)]
18(B1)→24(A1)	8.69	0	−257	0	σ*[H_2Se a_1: $4p_x$(Se)]
Me_2Se					
24(B2)→53(B1)	18.38	−151	0	0	–[e]
25(A1)→27(B2)	8.11	0	0	−622	σ*[Me_2Se b_2; $4p_y$(Se)]
25(A1)→32(B2)	9.82	0	0	−323	σ*[Me_2Se b_2; $4p_y$(Se)]
25(A1)→53(B1)	17.24	0	−159	0	σ*[Me_2Se a_1; $4p_x$(Se)]
26(B1)→27(B2)	5.55	−1161	0	0	σ*[Me_2Se b_2; $4p_y$(Se)]
26(B1)→28(A1)	5.66	0	−300	0	–[e]
26(B1)→32(B2)	7.26	−396	0	0	σ*[Me_2Se b_2; $4p_y$(Se)]
26(B1)→38(A1)	8.64	0	−213	0	σ*[Me_2Se a_1; $4p_y$(Se)]
Et_2Se					
32(B2)→36(A1)	8.56	0	0	−139	–[e]
33(A1)→35(B2)	7.76	0	0	−315	σ*[Et_2Se b_2: $4p_y$(Se)]
33(A1)→38(B2)	8.83	0	0	−313	σ*[Et_2Se b_2: $4p_y$(Se)]
34(B1)→35(B2)	5.43	−875	0	0	σ*[Et_2Se b_2: $4p_y$(Se)]
34(B1)→36(A1)	5.61	0	−179	0	–[e]
34(B1)→38(B2)	6.50	−530	0	0	σ*[Et_2Se b_2: $4p_y$(Se)]
34(B1)→42(A1)	7.06	0	−302	0	–[e]

[a] A utility program of Gaussian 03 (NMRANAL-NH03G) was applied, similarly to the cases in Table 3. [b] Values for $\sigma^p(Se)_{xx}$, $\sigma^p(Se)_{yy}$, and $\sigma^p(Se)_{zz}$ are given in ppm. [c] Contributions larger than 120 ppm to $|\sigma^p(Se)_{xx}+\sigma^p(Se)_{yy}+\sigma^p(Se)_{zz}|$ are shown. [d] Contributions from 16(B2)→23(B1) and 17(A1)→23(B1) are −59 ($=\sigma^p(Se)_{xx}$) and −52 ppm ($=\sigma^p(Se)_{yy}$), respectively, where ψ_{23} could be called $5p_z$(Se). [e] Difficult to specify.

Origin of the pre-α effect: The pre-α effect is analyzed by employing σ^p(Se) and the components of H_2Se ($\Delta\sigma^p$(Se-pα: H_2Se) = σ^p(Se-pα: H_2Se) = σ^p(Se: H_2Se)/2). As shown in Table 3, HOMO−2 (ψ_{16}), HOMO−1 (ψ_{17}), and HOMO (ψ_{18}) of H_2Se are mainly constructed by $4p_y$(Se), $4p_x$(Se), and $4p_z$(Se), respectively.[28] The contributions of ψ_{16}, ψ_{17}, and ψ_{18} to σ^p(Se) are −246, −351, and −626 ppm, respectively. The sum of σ^p(Se) over ψ_{16}–ψ_{18} amounts to −1223 ppm, which is 98% of that summed over ψ_1–ψ_{18} (−1248 ppm). The results show that the pre-α effect in H_2Se substantially originates from the three MOs. The contributions of the $\psi_i \rightarrow \psi_j$ and $\psi_i \rightarrow \psi_a$ transitions to σ^p(Se: H_2Se) are 317 and −1248 ppm, respectively. Therefore, σ^p(Se-pα: H_2Se) of −466 ppm ((317–1248)/2 ppm) must come from the $\psi_i \rightarrow \psi_a$ transitions, especially from ψ_i of ψ_{16}, ψ_{17}, and ψ_{18}.

tively, separately for the $\psi_i \rightarrow \psi_j$,[27] $\psi_i \rightarrow \psi_a$, and $\psi_i \rightarrow \psi_{j+a}$ transitions for various selenides. In Tables 5 and 6 the contributions to σ^p(Se) from the *trans* (C_s) and *gauche* (g) conformers of propyl derivatives are given separately. The mechanisms of the pre-α, α, β, and γ effects are elucidated on the basis of MO theory.

Figure 1 depicts the $\psi_i \rightarrow \psi_a$ transitions in H_2Se, which are listed in Table 4. It explains well how the pre-α effect originates from the transitions under the control of the angular momentum operator. Since Se^{2-} was chosen as the standard, σ^p(Se-pα: H_2Se) is explained by the generation of double σ-

Table 5. Contributions from the $\psi_i \rightarrow \psi_j$, $\psi_i \rightarrow \psi_a$, and $\psi_i \rightarrow \psi_{j+a}$ transitions to σ^p(Se) and the β effect.[a–c]

	$\psi_i \rightarrow \psi_j$		$\psi_i \rightarrow \psi_a$		$\psi_i \rightarrow \psi_{j+a}$		Total[d]	
Compound	σ^p(Se)	$\Delta\sigma^p$(Se-β)	σ^p(Se)	$\Delta\sigma^p$(Se-β)	σ^p(Se)	$\Delta\sigma^p$(Se-β)	σ^t(Se)	$\Delta\sigma^t$(Se-β)
$MeSe^-$ (C_{3v})	395.2	0.0	−1531.0	0.0	−1135.8	0.0	1865.1	0.0
$EtSe^-$ (C_s)	181.3	−213.9	−1524.7	6.3	−1343.3	−207.5	1661.0	−204.1
i$PrSe^-$ (C_s)	−396.2	−395.7	−1088.9	221.1	−1485.1	−174.7	1524.6	−170.3
t$BuSe^-$ (C_s)	−623.2	−339.5	−963.5	189.2	−1586.7	−150.3	1429.5	−145.2
MeSeH (C_s)	357.6	0.0	−1512.6	0.0	−1155.0	0.0	1843.2	0.0
EtSeH (C_s)	299.9	−57.7	−1534.8	−22.2	−1235.0	−80.0	1765.1	−78.1
*i*PrSeH (C_s)	195.9	−80.9	−1665.6	−76.5	−1469.7	−157.4	1534.8	−154.2
*i*PrSeH (C_1: *g*)	209.3	−74.2	−1620.7	−54.1	−1411.4	−128.2	1592.6	−125.3
*t*BuSeH (C_s)	30.1	−109.2	−1583.6	−23.7	−1553.5	−132.8	1455.8	−129.1
MeSeMe (C_{2v})	391.8	0.0	−1740.8	0.0	−1349.0	0.0	1650.1	0.0
MeSeEt (C_s)	319.7	−72.1	−1742.2	−1.4	−1422.5	−73.5	1579.4	−70.7
MeSeEt (C_1: *g*)	317.6	−74.2	1796.6	−55.8	−1479.0	−130.0	1523.0	−127.1
MeSe*i*Pr (C_1: *g*)	213.9	−89.0	−1765.9	−25.1	−1552.0	−101.5	1454.3	−97.9
MeSe*t*Bu (C_s)	84.7	−102.4	−1736.2	4.6	−1651.5	−100.8	1360.0	−96.7
EtSeEt (C_{2v})	175.4	−108.2	−1692.0	24.4	−1516.6	−83.8	1489.6	−80.3
EtSeEt (C_2)	268.9	−61.5	−1882.7	−71.0	−1613.8	−132.4	1390.3	−129.9
iPr_2Se (C_2)	−38.3	−107.5	−1738.8	0.5	−1777.1	−107.0	1238.2	−103.0
tBu_2Se (C_2)	−277.7	−115.6	−1693.0	8.0	−1970.7	−103.6	1056.4	−99.0

[a] Calculated with the 6-311+G(3df) basis set for Se and the 6-311+G(3d,2p) basis set for other nuclei of Gaussian 03 by using the GIAO-DFT method. [b] In ppm. [c] Given for a methyl group. [d] $\sigma^t(Se) = \sigma^p(Se) + \sigma^d(Se)$.

Table 6. Contributions from the $\psi_i \rightarrow \psi_j$, $\psi_i \rightarrow \psi_a$, and $\psi_i \rightarrow \psi_{j+a}$ transitions to σ^p(Se) and the γ effect.[a-c]

	$\psi_i \rightarrow \psi_j$		$\psi_i \rightarrow \psi_a$		$\psi_i \rightarrow \psi_{j+a}$		Total[d]	
Compound	σ^p(Se)	$\Delta\sigma^p$(Se-γ)	σ^p(Se)	$\Delta\sigma^p$(Se-γ)	σ^p(Se)	$\Delta\sigma^p$(Se-γ)	σ^t(Se)	$\Delta\sigma^t$(Se-γ)
EtSe$^-$ (C_s)	181.3	0.0	−1524.7	0.0	−1343.3	0.0	1661.0	0.0
*n*PrSe$^-$ (C_s)	248.9	67.6	−1546.7	−22.0	−1297.8	45.5	1706.2	45.2
*n*PrSe$^-$ (C_1: *g*)	282.3	101.0	−1514.8	9.9	−1232.5	110.8	1771.4	110.4
EtSeH (C_s)	299.9	0.0	−1534.8	0.0	−1235.0	0.0	1765.1	0.0
*n*PrSeH (C_s)	257.2	−42.7	−1478.0	56.8	−1220.8	14.2	1780.5	15.4
*n*PrSeH (C_1: *g*)	293.4	−6.5	−1507.4	27.4	−1214.0	21.0	1786.4	21.3
EtSeMe (C_s)	319.7	0.0	−1742.2	0.0	−1422.4	0.0	1579.4	0.0
*n*PrSeMe (C_s)	298.5	−21.2	−1706.7	35.5	−1408.2	14.2	1594.9	15.2
*n*PrSeMe (C_1: *g*)	352.1	32.4	−1746.5	−4.3	−1394.4	28.0	1607.9	28.5
*n*PrSeMe (C_1: *gg*)	332.8	13.1	−1724.8	17.4	−1392.0	30.4	1610.4	31.0
Et_2Se (C_{2v})	175.4	0.0	−1692.0	0.0	−1516.6	0.0	1489.6	0.0
nPr_2Se (C_{2v})	172.9	−1.3	−1662.2	14.9	−1489.3	13.7	1519.7	15.1
nPr_2Se (C_2: *gg*)	291.6	58.1	−1754.0	−31.0	−1462.4	27.1	1543.7	27.1
*n*BuSe$^-$ (C_s)[e]	209.5	−39.4	−1496.0	50.7	−1286.5	11.3	1718.0	11.8
*n*BuSeH (C_s)[e]	234.3	−22.9	−1454.4	23.6	−1220.1	0.7	1781.8	1.3
nBu_2Se (C_{2v})[e]	186.7	6.9	−1678.9	−8.4	−1492.2	−1.5	1519.8	0.1

[a] Calculated with the 6-311+G(3df) basis set for Se and the 6-311+G(3d,2p) basis set for other nuclei of Gaussian 03 by using the GIAO-DFT method. [b] In ppm. [c] Given for a methyl group. [d] $\sigma^t(Se) = \sigma^p(Se) + \sigma^d(Se)$. [e] Evaluated for $\Delta\sigma$(Se-δ).

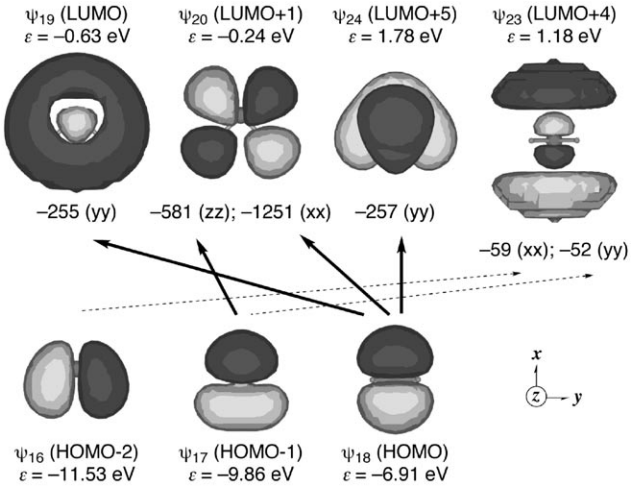

Figure 1. Contributions from each $\psi_i \rightarrow \psi_a$ transition to the components of σ^p(Se) in H_2Se. ψ_{16} and ψ_{23} are depicted for convenience of discussion, although their contributions are small. ψ_{18} and ψ_{23} are drawn from another direction.

(Se–H) and σ*(Se–H) through protonation at the spherical Se^{2-} ion. The four orbitals practically act as σ(H_2Se: a_1), σ(H_2Se: b_2), σ*(H_2Se: a_1), and σ*(H_2Se: b_2). They lead to effective $\psi_i \rightarrow \psi_a$ transitions, together with n_p(Se) of $4p_z$(Se), from which the pre-α effect in H_2Se mainly arises.

α effect: The analysis of the α effect is exemplified for Me_2Se by employing σ^p(Se) and the components listed in Table 3 ($\Delta\sigma^p$(Se-α: Me_2Se) = [σ^p(Se: Me_2Se) − σ^p(Se: H_2Se)]/2). Since atomic $4p_x$(Se), $4p_y$(Se), and $4p_z$(Se) orbitals interact with the local orbitals of the two Me groups in Me_2Se, the 4p(Se) character spreads over the whole molecule. The interactions result in the formation of HOMO−2 (ψ_{24}), HOMO−1 (ψ_{25}), and HOMO (ψ_{26}), which are mainly constructed by $4p_y$(Se), $4p_x$(Se), and $4p_z$(Se), respectively, together with ψ_{20}, ψ_{21}, and ψ_{22} with smaller contributions of $4p_x$(Se), $4p_z$(Se), and $4p_y$(Se), respectively.[29] The 4p(Se) character is also distributed to the unoccupied MOs, to a greater or lesser extent. Consequently, many $\psi_i \rightarrow \psi_a$ transitions contribute to σ^p(Se: Me_2Se).

The sums of σ^p(Se: Me_2Se) over ψ_{24}–ψ_{26} and ψ_{20}–ψ_{22} are −1535 and −192 ppm, respectively, which are 88 and 11% of the sum over ψ_1–ψ_{26} (−1741 ppm). On the other hand, the contribution from the $\psi_i \rightarrow \psi_j$ transitions to σ^p(Se: Me_2Se) is 392 ppm, which is larger than σ^p(Se: H_2Se) by 75 ppm. Therefore, the $\psi_i \rightarrow \psi_a$ transitions must contribute to $\Delta\sigma^p$(Se-α: Me_2Se). Figure 2 depicts the main $\psi_i \rightarrow \psi_a$ transitions, contributing to $\sigma^p(Se)_{xx}$, $\sigma^p(Se)_{yy}$, and $\sigma^p(Se)_{zz}$ in Me_2Se (see also Table 4). It explains how the α effect in Me_2Se originates from the transitions.

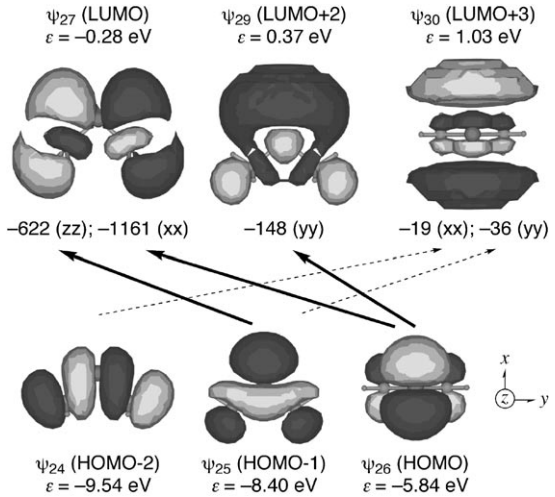

Figure 2. Contributions from each $\psi_i \rightarrow \psi_a$ transition to the components of σ^p(Se) in Me_2Se. ψ_{24} and ψ_{30} are depicted for convenience of discussion, although their contributions are small. ψ_{26} and ψ_{30} are drawn from another direction.

The α effect is the downfield shift caused by the replacement of Se–H by Se–Me. This replacement makes the electronic distribution around Se more unsymmetrical by changing the nature of the bond from 4p(Se)–1s(H) to 4p(Se)–2p(C), which must result in the larger downfield shift for Me_2Se relative to H_2Se. The replacement also affects the orbital energies. The increased values of the reciprocal orbital energy gaps $(\varepsilon_a-\varepsilon_i)^{-1}$ in Me_2Se relative to H_2Se must contribute to the downfield shift of Me_2Se.[30]

β effect: The β effect is predicted to be −84 ppm for Et_2Se ($\Delta\sigma^p$(Se-β: Et_2Se)=[σ^p(Se: Et_2Se)−σ^p(Se: Me_2Se)]/2) (Table 5). It is more difficult to understand the β effect intuitively on the basis of MO theory than is the case for the pre-α and α effects. The $\psi_i\rightarrow\psi_a$ transitions do not contribute to the β effect in Et_2Se, since the contributions to σ^p(Se: Et_2Se) and σ^p(Se: Me_2Se) from the $\psi_i\rightarrow\psi_a$ transitions are −1692 and −1741 ppm, respectively (Table 5). σ^p(Se: Et_2Se) is larger than σ^p(Se: Me_2Se) by 49 ppm, which is exactly the opposite trend to the β effect if the $\psi_i\rightarrow\psi_a$ transitions are considered. Instead, the contributions from the $\psi_i\rightarrow\psi_j$ transitions to σ^p(Se: Et_2Se) and σ^p(Se: Me_2Se) are 175 and 392 ppm, respectively. The former is smaller than the latter by 217 ppm, and this contributes to the β effect of −109 ppm, although they are both positive, that is, the β effect in Et_2Se is controlled by the $\psi_i\rightarrow\psi_j$ transitions. The positive value of σ^p(Se: Me_2Se) becomes smaller on substitution of the methyl proton(s) in Me_2Se by the Me group(s).

Is the β effect in usual selenides really controlled by the $\psi_i\rightarrow\psi_j$ transitions? As shown in Table 5, the $\psi_i\rightarrow\psi_j$ and $\psi_i\rightarrow\psi_a$ transitions contribute to the β effect by −116 to −58 ppm and −77 to 24 ppm, respectively, on the σ^p scale, for the nonionic species. The $\psi_i\rightarrow\psi_{j+a}$ transitions contribute −157 to −74 ppm, although the values depend on the structures. The main factor controlling the β effect is demonstrated to be the $\psi_i\rightarrow\psi_j$ transitions. The dependence of the β effect on conformation is also elucidated. The β effect is larger for *i*PrSeH of C_s symmetry [*i*PrSeH (C_s)] (−157 ppm) than that for EtSeH (C_s) (−80 ppm), which implies that the effect is much larger for the Me (*g*) group. The additivity rule seems to hold in the β effect. The value for *t*BuSeH (−133 ppm) is very close to the weighted average between EtSeH and *i*PrSeH (−131 ppm).

What happens when H of Me_2Se is replaced by Me? Figure 3 shows ψ_{32}–ψ_{34} in Et_2Se (C_{2v}). While ψ_{34} is mainly localized on the CH_2SeCH_2 framework of Et_2Se, ψ_{33} and ψ_{32} extend over the whole molecule of Et_2Se, with ψ_{32} delocalized more completely (Table 3).

What orbitals and transitions control the β effect? Their analysis is exemplified by Et_2Se (C_{2v}). The characters of ψ_{32} (HOMO−2), ψ_{33} (HOMO−1), and ψ_{34} (HOMO) in Et_2Se (C_{2v}) are σ[b_2: $4p_y$(Se)], σ[a_1: $4p_x$(Se)], and n_p[$4p_z$(Se)], respectively. Table 7 lists the contributions to $\sigma^p(Se)_{xx}$, $\sigma^p(Se)_{yy}$, and $\sigma^p(Se)_{zz}$ from the $\psi_i\rightarrow\psi_j$ transitions for ψ_i of HOMO, HOMO−1, and HOMO−2 and ψ_j of HOMO, HOMO−1, and HOMO−2, together with some important orbitals, in Me_2Se and Et_2Se. The contribution to the downfield shifts in

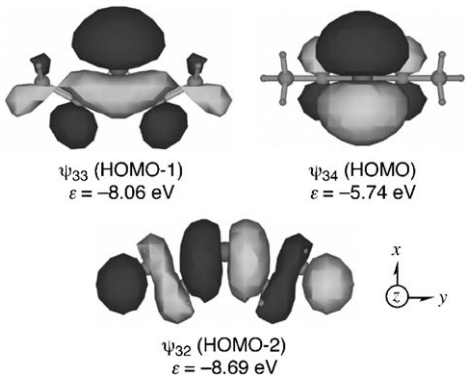

Figure 3. ψ_{32} (HOMO−2) of σ[b_2: $4p_y$(Se)], ψ_{33} (HOMO−1) of σ[a_1: $4p_x$(Se)], and ψ_{34} (HOMO) of n_p[$4p_z$(Se)] in Et_2Se of C_{2v} symmetry. ψ_{34} is drawn from another direction.

Table 7. Contributions to $\sigma^p(Se)_{xx}+\sigma^p(Se)_{yy}+\sigma^p(Se)_{zz}$ from some $\psi_i\rightarrow\psi_j$ transitions in Me_2Se and Et_2Se.[a,b]

ψ_i	ψ_j=	ψ_{20}	ψ_{21}	ψ_{22}	ψ_{24}	ψ_{25}	ψ_{26}	Sub-total	Δ[c]
Me_2Se (C_{2v})									
ψ_{26} (HOMO)		2	0	−5	−33	−33	0	−69	0
ψ_{25} (HOMO−1)		0	−16	183	856	0	721	1744	0
ψ_{24} (HOMO−2)		0	−74	0	0	−38	730	618	0
ψ_i	ψ_j=	ψ_{26}	ψ_{28}	ψ_{30}	ψ_{32}	ψ_{33}	ψ_{34}	Sub-total	Δ[c]
Et_2Se (C_{2v})									
ψ_{34} (HOMO)		−19	−3	0	−4	−24	0	−50	19
ψ_{33} (HOMO−1)		695	0	−58	370	0	521	1528	−216
ψ_{32} (HOMO−2)		0	2	−57	0	−16	84	13	−605

[a] By applying the utility program NMRANAL-NH98G. [b] In ppm. [c] σ^p(Se: R_2Se)−σ^p(Se: Me_2Se) for HOMO, HOMO−1, and HOMO−2, where R=Me or Et.

Et_2Se relative to Me_2Se is largest in HOMO−2. The difference of −605 ppm corresponds to the β effect of −101 ppm [−605/(3×2)]. The most important transition in the β effect is that from HOMO−2 to HOMO. The ψ_{24} (HOMO−2)→ψ_{26} (HOMO) transition contributes to the components of σ^p(Se) by 730 ppm in Me_2Se, whereas the corresponding ψ_{32} (HOMO−2)→ψ_{34}(HOMO) transition does so by 84 ppm in Et_2Se. The difference is −646 ppm, which generates the β effect of −108 ppm (−646/(3×2) ppm). The extension of ψ_{32} [b_2: $4p_y$(Se)] in Et_2Se over the whole molecule would be responsible for the smaller upfield shift in the transition to the HOMO (see Figure 3).

γ effect: Upfield shifts of 14 and 27 ppm are predicted from the $\psi_i\rightarrow\psi_{j+a}$ transitions for *n*Pr_2Se (C_{2v}) and *n*Pr_2Se (C_2: *gg*), respectively, relative to Et_2Se (C_{2v}) (Table 6), which correspond to the γ effect ($\Delta\sigma^p$(Se-γ: *n*Pr_2Se)=[σ^p(Se: *n*Pr_2Se)−σ^p(Se: Et_2Se)]/2). Although the upfield nature of $\Delta\sigma^p$(Se-γ) is suggested in both C_s (*trans*) and *g* conformers in *n*PrSeR, the mechanism seems complex. The $\psi_i\rightarrow\psi_a$ transition mainly contributes to the γ effect in *n*Pr_2Se (C_{2v}), whereas the $\psi_i\rightarrow\psi_j$ transition is responsible in *n*Pr_2Se (C_2: *gg*). A similar trend is observed in *n*PrSeMe. These results

imply that the $\psi_i \rightarrow \psi_a$ and $\psi_i \rightarrow \psi_j$ transitions mainly contribute to $\Delta\sigma^p$(Se-γ) in *n*PrSeR (C_s) and *n*PrSeR (*g*), respectively.

The relation between the contributions of $\psi_i \rightarrow \psi_a$ and $\psi_i \rightarrow \psi_j$ transitions was examined. Figure 4 shows a plot of

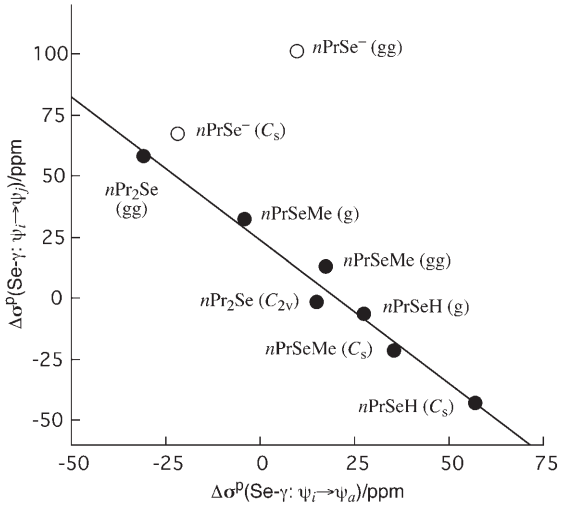

Figure 4. Plots of $\Delta\sigma^p$(Se-γ: $\psi_i \rightarrow \psi_j$) versus $\Delta\sigma^p$(Se-γ: $\psi_i \rightarrow \psi_a$) for *n*PrSeR (R = H, Me, and *n*Pr) and *n*PrSe$^-$, in various conformers.

the contributions to $\Delta\sigma^p$(Se-γ) from the $\psi_i \rightarrow \psi_j$ transitions [$\Delta\sigma^p$(Se-γ: $\psi_i \rightarrow \psi_j$)] versus $\Delta\sigma^p$(Se-γ: $\psi_i \rightarrow \psi_a$) for *n*PrSeR (R = H, Me, and *n*Pr). Equation (8) gives the correlation, which is fairly good ($r = 0.986$). The *y* intercept of the correlation (*b* in $y = ax + b$) is 24 ppm, which corresponds to the γ effect of the upfield shift for negligibly small $\Delta\sigma^p$(Se-γ: $\psi_i \rightarrow \psi_a$). The correlation constant of $a = -1.17$ is close to minus one. The results show that $\Delta\sigma^p$(Se-γ: $\psi_i \rightarrow \psi_j$) and $\Delta\sigma^p$(Se-γ: $\psi_i \rightarrow \psi_a$) will mostly cancel out, even if $\Delta\sigma^p$(Se-γ: $\psi_i \rightarrow \psi_a$) is not negligible. In this case, the γ effect will be more and less upfield than 24 ppm for $\Delta\sigma^p$(Se-γ: $\psi_i \rightarrow \psi_a$) < 0 and $\Delta\sigma^p$(Se-γ: $\psi_i \rightarrow \psi_a$) > 0, respectively. Such subtle balance between the contributions from the $\psi_i \rightarrow \psi_j$ and $\psi_i \rightarrow \psi_a$ transitions explains the small upfield shifts of the γ effect.[31]

$$\Delta\sigma^p(\text{Se-}\gamma:\ \psi_i \rightarrow \psi_j) = -1.17\,\Delta\sigma^p(\text{Se-}\gamma:\ \psi_i \rightarrow \psi_a) + 24.1 \quad (n = 7,\ r = 0.986) \tag{8}$$

The δ effect is negligibly small for *n*BuSeH and *n*Bu$_2$Se (Table 6). However, the contributions from the $\psi_i \rightarrow \psi_j$ and $\psi_i \rightarrow \psi_a$ transitions in *n*BuSeH (C_s) are −23 and 24 ppm relative to those in *n*PrSeH (C_s), respectively. The subtle balance between the two transitions also makes the effect very small.

The effect of p(Se)–π(C=C) conjugation is also important in δ(Se). The effect caused by ethenyl and phenyl groups was analyzed, together with the mechanism, in relation to the orientational effect.

Effect of p(Se)–π(C=C) conjugation: The replacement of Se−H by Se−CH=CH$_2$ induces p(Se)–π(C=C) conjugation, which causes a large downfield shift in δ(Se). The effect amounts to 300–500 ppm in ethenyl and phenyl selenides.[9] It is analyzed here for the examples of CH$_2$=CHSeR and PhSeR (R = H and Me).[22] Three conformers are considered for each of CH$_2$=CHSeR (R = H and Me), CH$_2$=CHSeR (**pl**-A), CH$_2$=CHSeR (**pl**-B), and CH$_2$=CHSeR (**pd**).[32] The **pl**-A conformer is predicted to be the global minimum for each.[33,34] Table 8 shows the effect of p(Se)–π(C=C) conjugation [$\Delta\sigma$(Se-π)] in ethenyl and phenyl selenides.

Table 8. Effect of p(Se)–π(C=C) conjugation, calculated and observed in ethenyl and phenyl selenides.[a-c]

Compound	σ^p(Se)	$\Delta\sigma^p$(Se-π)	σ^t(Se)	$\Delta\sigma^t$(Se-π)	σ^t(Se)[d]	$\Delta\sigma^t$(Se-π)[d]	δ(Se)[e]	Δδ(Se-π)[e]
Ethenyl effect								
HSeH	−931.3	0.0	2066.7	0.0	2252.7	0.0	−331.7	0.0
CH$_2$=CHSeH (**pl**-A)	−1426.7	−495.4	1574.3	−492.4	1824.3	−428.4		
CH$_2$=CHSeH (**pl**-B)	−1378.5	−447.2	1621.4	−445.3	1869.0	−383.7		
CH$_2$=CHSeH (**pd**)	−1315.7	−384.4	1685.1	−381.6	1917.8	−334.9		
Δ(**pl**-A−**pd**)[f]		−111.0		−110.6		−93.5		
Δ(**pl**-B−**pd**)[f]		−62.8		−63.7		−48.8		
HSeMe	−1155.0	0.0	1843.2	0.0	2072.7	0.0	−141.6	0.0
CH$_2$=CHSeMe (**pl**-A)	−1524.8	−369.8	1476.8	−366.4	1738.9	−333.8	186[g]	328[g]
CH$_2$=CHSeMe (**pl**-B)	−1525.3	−370.3	1476.7	−366.5	1744.6	−328.1		
CH$_2$=CHSeMe (**pd**)	−497.7	−342.7	1504.6	−338.6	1759.4	−313.3		
Δ(**pd**−**pl**-A)[f]		−27.1		−27.8		−20.5		
Δ(**pd**−**pl**-B)[f]		−27.6		−27.9		−14.8		
Phenyl effect								
HSeH	−931.3	0.0	2066.7	0.0	2251.3[h]	0.0	−331.7	0.0
PhSeH (**pl**)	−1436.1	−504.8	1563.4	−503.3	1801.5[h]	449.8	145	476.7
PhSeH (**pd**)	−1392.8	−461.5	1609.1	−457.6	1830.5[h]	420.8		
Δ(**pl**−**pd**)[f]		−43.3		−45.7		−29.0		
HSeMe	−1155.0	0.0	1843.2	0.0	2067.3[h]	0.0	−141.6	0.0
PhSeMe (**pl**)	−1525.8	−370.9	1480.7	−362.5	1727.5[h]	−339.8	202	343.6
PhSeMe (**pd**)	−1566.7	−411.7	1431.3	−411.9	1668.7[h]	−398.6		
Δ(**pl**−**pd**)[f]		40.9		49.4		58.8		

[a] Calculated with the 6-311+G(3df) basis set for Se and the 6-311+G(3d,2p) basis set for other nuclei of Gaussian 03. [b] In ppm. [c] By the GIAO-DFT method. [d] By the GIAO-MP2 method. [e] Observed values. [f] Corresponding to Δσ(Se-or). [g] Observed for *cis*-PhCH=CHSeMe. [h] Ref. [3d].

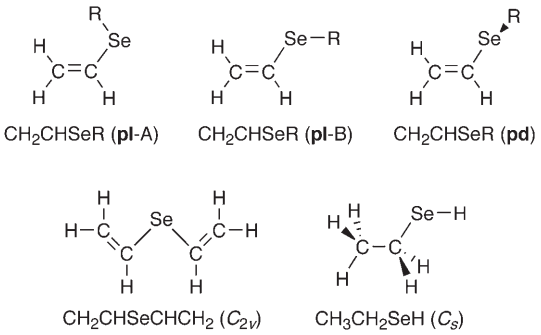

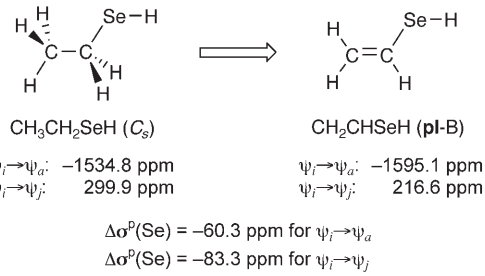

Scheme 3. Contributions of the $\psi_i \rightarrow \psi_a$ and $\psi_i \rightarrow \psi_j$ transitions in the formation of CH_2CHSeH (**pl**-B) from CH_3CH_2SeH (C_s).

The ethenyl effect on σ^p(Se) is predicted to be −495, −447, and −384 ppm for CH_2=CHSeH (**pl**-A), CH_2=CHSeH (**pl**-B), and CH_2=CHSeH (**pd**), respectively, and −370, −370, and −343 ppm for CH_2=CHSeMe (**pl**-A), CH_2=CHSeMe (**pl**-B), and CH_2=CHSeMe (**pd**), respectively, when calculated with the GIAO-DFT method (Table 8). Similarly, the effect for the former is −428, −384, and −335 ppm, respectively, and that for the latter is −334, −328, and −313 ppm, respectively, with the GIAO-MP2 method. The observed $\Delta\delta$(Se-π) value of *cis*-PhCH=CHSeMe (328 ppm) is very close to that calculated for CH_2=CHSeMe (**pl**) with the GIAO-MP2 method, although Ph is attached at the *cis* position in the observed compound.

The differences in σ(Se) between **pl** and **pd** conformers correspond to the orientational effects [$\Delta\sigma$(Se-or) = σ(Se: **pl**) − σ(Se: **pd**)]. The $\Delta\sigma^p$(Se-or) values predicted by the GIAO-DFT method increase in the order CH_2=CHSeH (A) (−111) < CH_2=CHSeH (B) (−63) < PhSeH (−43) < CH_2=CHSeMe (B) (−28) ≦ CH_2=CHSeMe (A) (−27) < PhSeMe (41 ppm). While $\Delta\sigma^p$(Se-or) are negative for both CH_2=CHSeH and CH_2=CHSeMe, those for PhSeH and PhSeMe are negative and positive, respectively. The replacement of Se−H by Se−Me increases $\Delta\sigma^p$(Se-or) for these compounds.

How is $\Delta\sigma^p$(Se-π) explained? We try to explain the effect with the formation of CH_2=CHSeH (**pl**-B) from CH_3CH_2SeH (C_s), where CH_2=CHSeH (**pl**-B) is related to CH_3CH_2SeH (C_s) by the elimination of H_2. While the $\psi_i \rightarrow \psi_j$ and $\psi_i \rightarrow \psi_a$ transitions make contributions to σ^p(Se) of CH_3CH_2SeH (C_s) of 300 and −1535 ppm, respectively, they contribute 217 and −1595 ppm, respectively, for CH_2=CHSeH (**pl**-B).[35] Scheme 3 summarizes the effect. The $\Delta\sigma^p$(Se-π: $\psi_i \rightarrow \psi_j$) and $\Delta\sigma^p$(Se-π: $\psi_i \rightarrow \psi_a$) values are −60 and −83 ppm, respectively (−143 ppm in $\psi_i \rightarrow \psi_{j+a}$). Both $\psi_i \rightarrow \psi_j$ and $\psi_i \rightarrow \psi_a$ transitions contribute to $\Delta\sigma^p$(Se-π) in almost equal magnitudes.

The importance of the $\psi_i \rightarrow \psi_j$ transitions, as well as the $\psi_i \rightarrow \psi_a$ transitions, is realized through the application of the utility program. The role of the $\psi_i \rightarrow \psi_j$ transitions and the behavior of atomic p orbitals are examined next.

Contributions of $\psi_i \rightarrow \psi_j$ and atomic p orbitals: Table 9 lists the contributions of p_x, p_y, and p_z to σ^p(Se) from the $\psi_i \rightarrow \psi_j$, $\psi_i \rightarrow \psi_a$ and $\psi_i \rightarrow \psi_{j+a}$ transitions in R_2Se (C_{2v}: R = H, Me, Et, *n*Pr, *n*Bu, and CH=CH_2)[36,37] and Se^{2-}, evaluated by using the utility program. Figure 5 depicts the contributions to σ^p(Se) from the $\psi_i \rightarrow \psi_j$, $\psi_i \rightarrow \psi_a$, and $\psi_i \rightarrow \psi_{j+a}$ transitions for the selenium species.

Atomic p orbitals contributing predominantly to σ^p(Se) are exhibited in Figure 5. The pre-α and α effects of the large downfield shifts are generated by the p($\psi \rightarrow \psi_a$) contributions, the β effect of the downfield shifts originates mainly through p($\psi_i \rightarrow \psi_j$), and the subtle balance between the $\psi_i \rightarrow \psi_j$ and $\psi_i \rightarrow \psi_a$ transitions controls the γ effect. The contributions from $p_x(\psi_i \rightarrow \psi_j)$, $p_y(\psi_i \rightarrow \psi_j)$, and $p_z(\psi_i \rightarrow \psi_j)$ are also depicted in Figure 5. The contributions from p($\psi_i \rightarrow \psi_j$) in the processes leading from Se^{2-} to H_2Se, Me_2Se, Et_2Se, and finally nPr_2Se are mainly controlled by $p_x(\psi_i \rightarrow \psi_j)$, $p_x(\psi_i \rightarrow \psi_j)$, $p_y(\psi_i \rightarrow \psi_j)$, and $p_z(\psi_i \rightarrow \psi_j)$, respectively. The β effect is mainly controlled by $p_y(\psi_i \rightarrow \psi_j)$. The transitions contributing to the pre-α, α, β, and γ effects are well visualized in Figure 5.

How do the atomic p orbitals p_x, p_y, and p_z contribute to the effects? The total contributions of p_x, p_y, and p_z were plotted versus those of p (= $p_x + p_y + p_z$). The (*a*, *r*) values in

Table 9. Contributions of p_x, p_y, and p_z to σ^p(Se) in R_2Se (C_{2v}), evaluated separately for $\psi_i \rightarrow \psi_j$, $\psi_i \rightarrow \psi_a$, and $\psi_i \rightarrow \psi_{j+a}$ transitions.[a]

R	p_x			p_y			p_z			$p_x+p_y+p_z$		
	$\psi_i \rightarrow \psi_j$	$\psi_i \rightarrow \psi_a$	$\psi_i \rightarrow \psi_{j+a}$	$\psi_i \rightarrow \psi_j$	$\psi_i \rightarrow \psi_a$	$\psi_i \rightarrow \psi_{j+a}$	$\psi_i \rightarrow \psi_j$	$\psi_i \rightarrow \psi_a$	$\psi_i \rightarrow \psi_{j+a}$	$\psi_i \rightarrow \psi_j$	$\psi_i \rightarrow \psi_a$	$\psi_i \rightarrow \psi_{j+a}$
Se^{2-}[b]	0	0	0	0	0	0	0	0	0	0	0	0
H	128	−373	−245	−121	−254	−375	343	−632	−289	350	−1259	−909
Me	319	−718	−397	−277	−235	−512	433	−839	−406	475	−1790	−1315
Et	257	−690	−433	−389	−209	−598	406	−861	−455	274	−1760	−1486
*n*Pr	313	−741	−428	−452	−128	−580	407	−854	−447	268	−1723	−1455
*n*Bu	287	−715	−428	−412	−168	−580	404	−856	−447	284	−1739	−1455
CH_2=CH[c]	389	−875	−486	−385	−222	−607	175	−752	−581	179	−1853	−1674

[a] Values are given in ppm. [b] R_2Se (C_{2v}) = Se^{2-} (O_h). [c] σ^p(Se) = −1720.7 ppm.

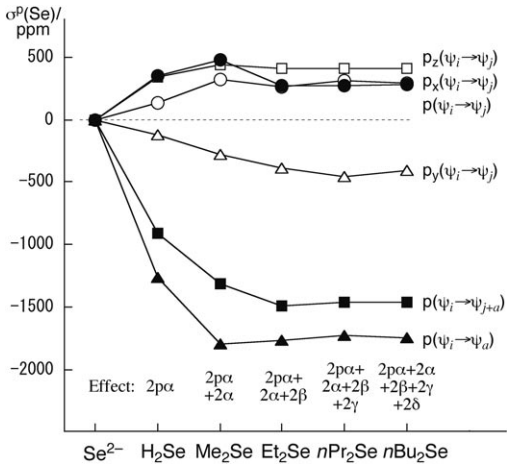

Figure 5. Contributions from the $\psi_i \rightarrow \psi_j$ (●), $\psi_i \rightarrow \psi_a$ (▲), $\psi_i \rightarrow \psi_{j+a}$ (■) transitions for p ($=p_x+p_y+p_z$), together with the $\psi_i \rightarrow \psi_j$ transitions for p_x (○), p_y (△), and p_z (□) to σ^p(Se) in Se^{2-} (O_h) and R_2Se (C_{2v}: R = H, Me, Et, *i*Pr, and *i*Bu).

the correlations ($y = ax + b$, r) were (0.297, 0.998), (0.397, 0.999), and (0.306, 1.000) for p_x, p_y, and p_z, respectively (not shown). The correlation constants are in the order of $a(p_y) > a(p_z) \cong a(p_x)$. Atomic $4p_x$(Se), $4p_y$(Se), and $4p_z$(Se) orbitals construct $\sigma(R_2Se: a_1)$ of n_s(Se), $\sigma(R_2Se: b_2)$, and n_p(Se) in R_2Se (C_{2v}), respectively. $\sigma(R_2Se: b_2)$ of $4p_y$(Se) tends to extend over the whole molecule, and would thus be responsible for the largest contribution. The results are consistent with the large contribution from the HOMO−2 (p_y)→ HOMO (p_z) transition in the β effect in Et_2Se.

These considerations are supported by the highly extended molecular π orbitals in CH_2=CHSeCH=CH_2 (C_{2v}) constructed by p_z. The contributions from p_x, p_y, and p_z to σ^p(Se) are −486, −607, and −581 ppm, respectively, the ratio of which is 0.290:0.363:0.347. The increased contribution from p_z must be the result of the extended p_z character over the whole molecule in π(C=C−Se−C=C).

By means of the proposed pre-α effect, δ(Se) are analyzed and well understood in a unified style. The importance of the $\psi_i \rightarrow \psi_j$ transitions is realized through the application of the utility program.

Conclusion

How do δ(Se) originate in dependence on the structures of selenium compounds? The origin has been clarified on the basis of MO theory, as a first step to establishing plain rules founded in the theoretical background, which are necessary to understand the origin of δ(Se) in the structures. A utility program derived from Gaussian 03 (NMRANAL-NH03G) was applied for the analysis. The concept of pre-α effect is proposed, which is defined as the downfield shift due to attachment of a proton to a lone-pair orbital of Se. The pre-α effect in H_2Se is explained by the generation of double σ(Se−H) and σ*(Se−H) by the addition of protons at spherical Se^{2-}, since Se^{2-} was chosen as standard. The double σ(Se−H) and σ*(Se−H) orbitals practically act as $\sigma(H_2Se: a_1)$, $\sigma(H_2Se: b_2)$, $\sigma^*(H_2Se: a_1)$, and $\sigma^*(H_2Se: b_2)$ in H_2Se, which leads to effective $\psi_i \rightarrow \psi_a$ transitions, together with n_p(Se). The α effect is the downfield shift caused by the replacement of Se−H with Se−Me. The $\psi_i \rightarrow \psi_a$ transitions in ψ_{24} [HOMO−2: $4p_y$(Se)], ψ_{25} [HOMO−1: $4p_x$(Se)], and ψ_{26} [HOMO: $4p_z$(Se)] of Me_2Se must be responsible for the effect. The β effect seems more complex to understand intuitively based on MO theory than is the case for the pre-α and α effects. The $\psi_i \rightarrow \psi_a$ transitions do not contribute to the β effect, but the $\psi_i \rightarrow \psi_j$ transitions do. Although the $\psi_i \rightarrow \psi_j$ transitions are usually positive, the positive value in Me_2Se becomes smaller and then negative when the methyl protons in Me_2Se are successively substituted by Me groups. The γ effect is more complex. The upfield shift is derived from the well-balanced contributions from the $\psi_i \rightarrow \psi_j$ and $\psi_i \rightarrow \psi_a$ transitions. A similar subtle balance makes the δ effect very small. The effect of the p(Se)–π(C=C) conjugation is also derived from a subtle balance. The results presented here will help understand the origin of δ(Se), even for experimental chemists.

Investigations to evaluate the electron population factor $\langle r^{-3} \rangle$ are in progress. The results, as well as applications, will be reported elsewhere.

Acknowledgements

This work was partially supported by a Grant-in-Aid for Scientific Research from the Ministry of Education, Culture, Sports, Science, and Technology, Japan (No. 16550038).

[1] a) *Encyclopedia of Nuclear Magnetic Resonance* (Eds.: D. M. Grant, R. K. Harris), Wiley, New York, **1996**; b) *Nuclear Magnetic Shieldings and Molecular Structure* (Ed.: J. A. Tossell), Kluwer Academic, Dordrecht, **1993**; c) *Calculation of NMR and EPR Parameters; Theory and Applications* (Eds.: M. Kaupp, M. Bühl, V. G. Malkin), Wiley-VCH, Weinheim, **2004**; d) *Spins in Chemistry* (Ed.: R. McWeeny), Academic Press, New York, **1970**; e) V. G. Markin, O. L. Malkina, L. A. Eriksson, "*A Tool for Chemistry*" in *Modern Density Functional Theory* (Eds.: J. M. Seminario, P. Politzer), Elsevier, Amsterdam, **1994**; f) *Density-functional Methods in Chemistry and Material Science* (Ed.: M. Springborg), Wiley, New York, **1977**.

[2] a) *Organic Selenium Compounds: Their Chemistry and Biology* (Eds.: D. L. Klayman, W. H. H. Günther), Wiley, New York, **1973**; b) *The Chemistry of Organic Selenium and Tellurium Compounds, Vols. 1 and 2* (Eds.: S. Patai, Z. Rappoport), Wiley, New York, **1986**; c) *Organic Selenium Chemistry* (Ed.: D. Liotta), Wiley-Interscience, New York, **1987**; d) *Organoselenium Chemistry, A Practical Approach* (Ed.: T. G. Back), Oxford University Press, Oxford, **1999**; e) *Organoselenium Chemistry Modern Developments in Organic Synthesis, Top. Curr. Chem., Vol. 208* (Ed.: T. Wirth), Springer, Heidelberg, **2000**.

[3] a) W. MacFarlane, R. J. Wood, *J. Chem. Soc. Dalton Trans.* **1972**, *13*, 1397–1401; b) H. Iwamura, W. Nakanishi, *J. Syn. Org. Chem. Jpn.* **1981**, *39*, 795–804; c) *The Chemistry of Organic Selenium and Tellurium Compounds, Vol. 1* (Eds.: S. Patai, Z. Rappoport), Wiley, **1986**, Chap. 6; d) *Compilation of Reported ^{77}Se NMR Chemical Shifts* (Eds.: T. M. Klapotke, M. Broschag), Wiley, New York, **1996**; e) H. Duddeck, *Prog. Nucl. Magn. Reson. Spectrosc.* **1995**, *27*, 1–323.

[4] a) S. Gronowitz, A. Konar, A.-B. Hörnfeldt, *Org. Mag. Res.* **1977**, *9*, 213–217; b) G. P. Mullen, N. P. Luthra, R. B. Dunlap, J. D. Odom, *J.*

Org. Chem. **1985**, *50*, 811–816; c) G. A. Kalabin, D. F. Kushnarev, V. M. Bzesovsky, G. A. Tschmutova, *J. Org. Mag. Res.* **1979**, *12*, 598–604; d) G. A. Kalabin, D. F. Kushnarev, T. G. Mannafov, *Zh. Org. Khim.* **1980**, *16*, 505–512; e) W. Nakanishi, S. Hayashi, T. Uehara, *Eur. J. Org. Chem.* **2001**, 3933–3943.

[5] a) S. Hayashi, W. Nakanishi, *J. Org. Chem.* **1999**, *64*, 6688–6696; b) W. Nakanishi, S. Hayashi, H. Yamaguchi, *Chem. Lett.* **1996**, 947–948; c) W. Nakanishi, S. Hayashi, A. Sakaue, G. Ono, Y. Kawada, *J. Am. Chem. Soc.* **1998**, *120*, 3635–3640; d) W. Nakanishi, S. Hayashi, *J. Org. Chem.* **2002**, *67*, 38–48.

[6] a) W. Nakanishi, S. Hayashi, *Chem. Lett.* **1998**, 523–524; b) W. Nakanishi, S. Hayashi, *J. Phys. Chem. A* **1999**, *103*, 6074–6081.

[7] W. Nakanishi, S. Hayashi, D. Shimizu, M. Hada, *Chem. Eur. J.* **2006**, *12*, 3829–3846; S. Hayashi, W. Nakanishi, *Bioinorg. Chem. Appl.* **2006**, DOI: 10.1155/BCA/2006/23214, in press.

[8] Downfield shifts of about 110–170 and 100 ppm are observed for the α and β effects, respectively, although the values depend on the conditions of measurement, such as solvents (see Table 2).[3] The γ effect is an upfield shift of about 30 ppm.[3]

[9] The ethenyl and phenyl effects in the p(Se)–π(C=C) conjugation are reported to be downfield shifts of about 300 and 500 ppm, respectively.[3]

[10] Although the contribution of relativistic terms has been pointed out for heavier atoms, the perturbation would be small for the selenium nucleus: R. Fukuda, M. Hada, H. Nakatsuji, *J. Chem. Phys.* **2003**, *118*, 1015–1026; R. Fukuda, M. Hada, H. Nakatsuji, *J. Chem. Phys.* **2003**, *118*, 1027–1035; S. Tanaka, M. Sugimoto, H. Takashima, M. Hada, H. Nakatsuji, *Bull. Chem. Soc. Jpn.* **1996**, *69*, 953–959; C. C. Ballard, M. Hada, H. Kaneko, H. Nakatsuji, *Chem. Phys. Lett.* **1996**, *254*, 170–178; H. Nakatsuji, M. Hada, H. Kaneko, C. C. Ballard, *Chem. Phys. Lett.* **1996**, *255*, 195–202; M. Hada, H. Kaneko, H. Nakatsuji, *Chem. Phys. Lett.* **1996**, *261*, 7–12.

[11] a) K. Kanda, H. Nakatsuji, T. Yonezawa, *J. Am. Chem. Soc.* **1984**, *106*, 5888–5892; b) *Molecular Quantum Mechanics*, 3rd ed. (Eds.: P. W. Atkins, R. S. Friedman), Oxford, New York, **1997**, Chap. 13.

[12] This decomposition includes a small degree of arbitrariness due to the dependence on coordinate origin, though it is not detrimental to our chemical analyses and insights into ^{77}Se NMR spectroscopy.

[13] The transition from occupied orbitals (ψ_i) to unoccupied orbitals (ψ_a) mainly contributes to $\boldsymbol{\sigma}^{p}$. However, that from occupied orbitals (ψ_i) to occupied orbitals (ψ_j) sometimes play an important role in $\boldsymbol{\sigma}^{p}$. Such typical cases are detected in the β effect.

[14] $\boldsymbol{\sigma}^{p}$ and $\boldsymbol{\sigma}^{d}$ are exactly expressed by Ramsey's Equation, and they are approximately calculated in the framework of Hartree–Fock (HF) or DFT theory: N. F. Ramsey, *Phys. Rev.* **1949**, *77*, 567–575; N. F. Ramsey, *Phys. Rev.* **1950**, *78*, 699–703; N. F. Ramsey, *Phys. Rev.* **1951**, *83*, 540–541; N. F. Ramsey, *Phys. Rev.* **1952**, *85*, 143–144; N. F. Ramsey, *Phys. Rev.* **1953**, *91*, 303–307; N. F. Ramsey, *Phys. Rev.* **1956**, *86*, 243–246.

[15] Based on second-order perturbation theory at the level of the HF and single-excitation CI approximation, $\boldsymbol{\sigma}^{p}_{i\rightarrow a}$ on a resonance nucleus N is shown to be proportional to reciprocal orbital energy gap $(\varepsilon_a-\varepsilon_i)^{-1}$ as expressed in Equation (5), where ψ_k is the k-th orbital function, $\hat{L}_{z,N}$ the orbital angular momentum around the resonance nucleus, and r_N the distance from the nucleus N.

[16] For a similar utility program based on Gaussian 98 (NMRANAL-NH98G), see ref. [7]. The contribution from orbital-to-orbital transitions is separately evaluated for i, j, and a in the $\psi_i\rightarrow\psi_j$ and $\psi_i\rightarrow\psi_a$ transitions in NMRANAL-NH98G. That in NMRANAL-NH03G is given after summation over i and j for the $\psi_i\rightarrow\psi_j$ transitions.

[17] Gaussian 03, Revision B.05, M. J. Frisch, G. W. Trucks, H. B. Schlegel, G. E. Scuseria, M. A. Robb, J. R. Cheeseman, J. A. Montgomery, Jr., T. Vreven, K. N. Kudin, J. C. Burant, J. M. Millam, S. S. Iyengar, J. Tomasi, V. Barone, B. Mennucci, M. Cossi, G. Scalmani, N. Rega, G. A. Petersson, H. Nakatsuji, M. Hada, M. Ehara, K. Toyota, R. Fukuda, J. Hasegawa, M. Ishida, T. Nakajima, Y. Honda, O. Kitao, H. Nakai, M. Klene, X. Li, J. E. Knox, H. P. Hratchian, J. B. Cross, V. Bakken, C. Adamo, J. Jaramillo, R. Gomperts, R. E. Stratmann, O. Yazyev, A. J. Austin, R. Cammi, C. Pomelli, J. W. Ochterski, P. Y. Ayala, K. Morokuma, G. A. Voth, P. Salvador, J. J. Dannenberg, V. G. Zakrzewski, S. Dapprich, A. D. Daniels, M. C. Strain, O. Farkas, D. K. Malick, A. D. Rabuck, K. Raghavachari, J. B. Foresman, J. V. Ortiz, Q. Cui, A. G. Baboul, S. Clifford, J. Cioslowski, B. B. Stefanov, G. Liu, A. Liashenko, P. Piskorz, I. Komaromi, R. L. Martin, D. J. Fox, T. Keith, M. A. Al-Laham, C. Y. Peng, A. Nanayakkara, M. Challacombe, P. M. W. Gill, B. Johnson, W. Chen, M. W. Wong, C. Gonzalez, J. A. Pople, Gaussian, Inc., Pittsburgh, PA, **2003**.

[18] a) A. D. Becke, *Phys. Rev. A* **1988**, *38*, 3098–3100; A. D. Becke, *J. Chem. Phys.* **1993**, *98*, 5648–5652; b) C. Lee, W. Yang, R. G. Parr, *Phys. Rev. B* **1988**, *37*, 785–789; B. Michlich, A. Savin, H. Stall, H. Preuss, *Chem. Phys. Lett.* **1989**, *157*, 200–2006.

[19] K. Wolinski, J. F. Hinton, P. Pulay, *J. Am. Chem. Soc.* **1990**, *112*, 8251–8260; K. Wolinski, A. Sadlej, *Mol. Phys.* **1980**, *41*, 1419–1430; R. Ditchfield, *Mol. Phys.* **1974**, *27*, 789–807; R. McWeeny, *Phys. Rev.* **1962**, *126*, 1028–1034; F. London, *J. Phys. Radium, Paris* **1937**, *8*, 397–409.

[20] C. Möller, M. S. Plesset, *Phys. Rev.* **1934**, *46*, 618–622; J. Gauss, *J. Chem. Phys.* **1993**, *99*, 3629–3643; J. Gauss, *Ber. Bunsenges, Phys. Chem.* **1995**, *99*, 1001–1008.

[21] For calculations of $\boldsymbol{\sigma}$(Se: H_2Se), see a) W. Kutzelnigg, U. Fleischer, C. van Wüllen, "*Shielding Calculations: IGLO Method*" in *Encyclopedia of Nuclear Magnetic Resonance*, *Vol. 7*, (Eds.: D. M. Grant, R. K. Harris), Wiley, New York, **1996**, 4284–4291; b) P. D. Ellis, J. D. Odom, A. S. Lipton, Q. Chen, J. M. Gulick, "*Gas Phase Measurement and ab initio Calculations*" in *Nuclear Magnetic Shieldings and Molecular Structure* (Ed.: J. A. Tossell), Kluwer Academic Publishers, Dordrecht, **1993**, 539–555; c) P. J. Wilson, *Mol. Phys.* **2001**, *99*, 363–367. See also ref. [7].

[22] The affect on $\boldsymbol{\sigma}^{t}$(Se) in PhSeH and PhSeMe is discussed in ref. [7]. The orientational effect is not so large between the two methods.

[23] We must be very careful when the observed δ(Se: Se^{2-}) is discussed. δ(Se: Se^{2-}) is reported to be −511 ppm,[24a] which is very close to δ(Se: NaSeH) in MeOH (−514 ppm)[24b] and close to δ(Se: $Me_4N^+SeH^-$) in the solid state (−465 ppm).[24b] δ(Se: NaSeH) changes to −393 ppm in DMF and to −529 ppm in H_2O.[24]

[24] a) J. D. Odom, W. H. Dawson, P. D. Ellis, *J. Am. Chem. Soc.* **1979**, *101*, 5815–5822; b) R. J. Batchelor, F. W. B. Einstein, I. D. Gay, C. H. W. Jones, R. D. Sharma, *Inorg. Chem.* **1993**, *32*, 4378; c) D. Rabinovich, G. Parkin, *Inorg. Chem.* **1993**, *32*, 4378–4383.

[25] The solvent effect on δ(Se: H_2Se) is also large: it is −331.7 ppm in the gas phase, whereas it is −226.8 ppm in $CDCl_3$ and −288 ppm in D_2O.

[26] Equation (9) shows the correlation of similar plots for the data in Tables 2 and 8, containing those for Se^{2-}, HSe^-, H_2Se, and H_3Se^+. The (a, r) values are (1.14, 0.997). The point for Se^{2-} deviates above the correlation line, that is, the pre-α effect evaluated with the GIAO-DFT method will be more than 1.14 times larger than that based on the GIAO-MP2 method. A similar trend is also suggested for the α effect.

$$\boldsymbol{\sigma}^{t}(\text{B3LYP}) = 1.141\,\boldsymbol{\sigma}^{t}(\text{MP2}) - 493.2 \quad (n=29,\ r=0.997) \qquad (9)$$

[27] The $\psi_i\rightarrow\psi_j$ transition should be described as $\psi_i\rightarrow\psi_j$ ($j\neq i$). However, we write it as $\psi_i\rightarrow\psi_j$, since the contribution from the $\psi_i\rightarrow\psi_i$ transition is intrinsically zero.

[28] In the case of H_2Se, ψ_{16}, ψ_{17}, and ψ_{18} are mainly constructed by $4p_y$(Se), $4p_x$(Se), and $4p_z$(Se), respectively; ψ_7, ψ_8, and ψ_9 by $3p_y$(Se), $3p_x$(Se), and $3p_z$(Se), respectively; and ψ_3, ψ_4, and ψ_5 by $2p_y$(Se), $2p_x$(Se), and $2p_z$(Se), respectively.

[29] The contributions of np_y(Se), np_x(Se), and np_z(Se) (n=2, 3, and 4) to ψ_i in Me_2Se are essentially the same as in the case of H_2Se, although ψ_6 and ψ_7 are constructed by two 1s(C).

[30] As expressed in Equation (5), $\boldsymbol{\sigma}^{p}$(Se) are mainly controlled by the reciprocal orbital energy gaps $(\varepsilon_j-\varepsilon_i)^{-1}$, the r_N^{-3} terms, and the overlap integrals containing the angular momentum operator $\hat{L}$.

[31] While the point corresponding to nPrSe$^-$ (C_s) is almost on the correlation line in Figure 4, that for nPrSe$^-$ (g) deviates above the line. This must be due to the very large upfield contribution from the $\psi_i\rightarrow\psi_j$ transition in nPrSe$^-$ (g).

[32] Since CH_2=CHSeH (**pd**) is not a minimum, the dihedral angle of C_2C_1SeH was fixed at 90.0° in the optimization. Calculations on CH_2=CHSeMe (**pd**) were performed similarly.

[33] The relative energies of CH_2=CHSeH (**pl**-A), CH_2=CHSeH (**pl**-B), and CH_2=CHSeH (**pd**)[32] are predicted to be 0.0, 0.4, and 7.9 kJ mol^{-1}, respectively, when calculated at the DFT level, and those of the first two are 0.0 and 1.0 kJ mol^{-1} at the MP2 level.

[34] The relative energies of CH_2=CHSeMe (**pl**-A), CH_2=CHSeMe (**pl**-B), and CH_2=CHSeMe (**pd**)[32] are 0.0, 7.9, and 14.7 kJ mol^{-1}, respectively, at the DFT level, and those of the first two are 0.0 and 7.4 kJ mol^{-1}, respectively, at the MP2 level.

[35] Table S1 in the Supporting Information collects the contributions from each ψ_i to σ^p(Se) and the components ($\sigma^p(Se)_{xx}$, $\sigma^p(Se)_{yy}$, and $\sigma^p(Se)_{zz}$) in CH_2=CHSeH (**pl**-A), CH_2=CHSeH (**pl**-B), CH_2=CHSeH (**pd**), and CH_3CH_2SeH (C_s), together with the energies (ε_i) and the characters of ψ_i.

[36] The $\psi_i \rightarrow \psi_{j+a}$ contributions to σ^p(Se) of these compounds, given in Table 9, are contributed from the atomic p, d, and f orbitals in the basis sets for the calculations.

[37] The $\psi_i \rightarrow \psi_{j+a}$ contributions from p ($=p_x+p_y+p_z$) in Table 9 were plotted versus those in Tables 2 and 6, which correspond the contributions from (p+d+f), for Se^{2-} and R_2Se (C_{2v}, R = H, Me, Et, *n*Pr, *n*Bu, and CH_2=CH). The correlation is given in Equation (10).

$$\sigma^p(p) = 0.976\,\sigma^p(p+d+f) - 0.3 \quad (n = 7, \quad r = 1.000) \qquad (10)$$

The correlation is obtained with more significant figures than those in the tables. The results show that atomic p orbitals in ψ_i are the origin of about 98% of σ^p(Se) ($a = 0.976$) by the basis sets in the calculations.

[38] D. Rabinovich, G. Parkin, *Inorg. Chem.* **1994**, *33*, 2313–2314.

[39] N. P. Luthra, R. B. Dunlap, J. D. Odom, *J. Magn. Reson.* **1983**, *52*, 318–322.

[40] N. P. Luthra, A. M. Boccanfuso, R. B. Dunlap, J. D. Odom, *J. Organomet. Chem.* **1988**, *354*, 51.

Received: December 13, 2006
Published online: April 16, 2007

